J Math Chem (2009) 46:427–442
DOI 10.1007/s10910-008-9468-2

ORIGINAL PAPER

Computational modelling of the YAG synthesis

Feliksas Ivanauskas · Aivaras Kareiva · Bogdan Lapcun

Received: 29 June 2008 / Accepted: 9 September 2008 / Published online: 9 October 2008

Abstract Mathematical and numerical models of the yttrium aluminium garnet (YAG) synthesis are presented in the article. The models allow the effective computer simulation of the YAG synthesis. The synthesis by sol–gel and solid-state reaction methods is considered in the article. The question concerning the reasons for the observed changes in the preparation temperature by changing synthesis method is answered. The inverse modelling problem is solved: using known experimental data (synthesis time, dimensions of reactants) the unknown input parameters of the model (diffusion and reaction rate coefficients) are calculated.

Keywords Yttrium aluminium garnet · Reaction–diffusion model

1 Introduction

The composition $3Y_2O_3 : 5Al_2O_3$, commonly called as yttrium aluminium garnet ($Y_3Al_5O_{12}$, YAG), adopts the cubic garnet structure and when doped with a transition metal or lanthanide element, YAG is an important solid-state laser material widely used in luminescence systems and window materials for a variety of lamps [1,3–7]. In view of the high-temperature chemical stability and an extremely high

F. Ivanauskas · B. Lapcun (✉)
Department of Mathematics and Informatics, Vilnius University, Naugarduko str. 24, Vilnius 03225, Lithuania
e-mail: blapcun@gmail.com

F. Ivanauskas
Institute of Mathematics and Informatics, Akademijos str. 4, Vilnius 08663, Lithuania

A. Kareiva
Department of Chemistry, Vilnius University, Naugarduko str. 24, Vilnius 03225, Lithuania

creep resistance, YAG is a promising fiber material for the preparation of ceramic composites [8,11,13–19,21]. The electrical conductivity of YAG is also reported to be lower than any other polycrystalline oxide [2]. Owing to such wide and diverse application potential of YAG-based ceramics, new routes for the synthesis of pure and homogeneously doped YAG are highly desirable.

The YAG powders could be synthesized by many different methods, such as solid-state reaction method, spray pyrolysis, coprecipitation, sol–gel and others [1,11,13,15,17,25,35–37]. The solid-state synthesis of YAG ceramic from Al_2O_3 and Y_2O_3 powders usually requires extensive mechanical mixing and lengthy heat treatments above 1600 °C [22,25]. These processing conditions do not allow facile control over microstructure, grain size and grain size distribution in the resulting powders or shapes. Several wet-chemical techniques such as polymerized complex route [15], metal–organic preceramic processing [22], coprecipitation methods [27,29] or yttrium carboxylate–alumoxane route [4] have been used to produce YAG phases. Most of these methods suffer from the complex and time consuming (long refluxing times, gelation periods of several days, etc.) procedures and/or mismatch in the solution behaviour of the constituents. As a consequence of the different isoelectric points, gross inhomogeneities may be present in the obtained ceramic, e.g., significant amounts of Y_2O_3, Al_2O_3, $YAlO_3$ and $Y_2Al_4O_9$ phases are present, even above 1650 °C, in the $Y_3Al_5O_{12}$ phase synthesized by above mentioned "soft chemistry" methods.

Recently, for the preparation of nanocrystalline YAG it has been developed a new sol–gel process using mixtures of inorganic salts of the respective elements [32]. The study have demonstrated the versatility of the sol–gel method to yield monophasic YAG samples at lower sintering temperature ($\approx$1000 °C) when compared to the temperature required for the solid-state synthesis (>1600 °C). The successful synthesis of crystalline YAG phase at 1000 °C is the one of the lowest reported temperature for the crystallisation of this material. The sol–gel method of preparation of YAG in aqueous media is inexpensive and thus appropriate for the large scale production of YAG ceramics. Also, lanthanide-doped YAG ceramics could be successfully obtained by sol–gel method.

Therefore, it has been well demonstrated that the sol–gel process offers considerable advantages of good mixing of the starting materials and excellent chemical homogeneity of the product. Moreover, the molecular level mixing and the tendency of partially hydrolyzed species to form extended networks facilitate the structure evolution thereby lowering the crystallization temperature. The reactivity of the precursor makes the preparation of particular phases possible at ambient and gentle conditions while starting from a solid-state precursor either high temperatures or high pressure or the use of a catalyst is needed.

Thus, it is clear that the conditions for the formation of monophasic YAG are dependent largely on the synthesis method used. By changing solid-state method to the sol–gel chemistry approach, the YAG formation temperature decreases from 1600 °C upto 1000 °C. However, the important question concerning the reasons for the observed changes in the preparation temperature by changing synthesis method remains to be answered. Such a situation has initiated the present work, motivating us to elucidate the reasons responsible for the low-temperature formation of $Y_3Al_5O_{12}$ using sol–gel technique. The optimization of synthesis parameters of sol–gel processes have been

determined mostly in an experimental way, i.e., according to the desired properties of the final ceramic material. To overcome these difficulties, the pathway of chemical reactions should be performed according to the possible computational modelling. However, no model has yet been constructed that provides quantitative agreement of the reaction mechanisms with the experimental data of process parameters and desired structural, morphological and physical properties of the final ceramic material.

The first goal of this study is to construct a mathematical model which allows the effective computer simulation of the YAG synthesis, and in particular, which allows us to determine the exact reasons responsible for the different formation temperatures of $Y_3Al_5O_{12}$ using different techniques. We have analyzed the YAG synthesis carried out by solid-state reaction and by sol–gel methods in this study. A mathematical model for the synthesis is presented in Sect. 3. Before, in Sect. 2, we describe the details and results of the laboratory experiments of the YAG synthesis using sol–gel and solid-state reaction methods at different temperatures.

The kinetics of solid-state reactions generally cannot be assumed to follow simple rate laws that are applicable to homogeneous reactions [33]. The rate of a general homogeneous reaction is conventionally measured by following the decrease in concentration of reactants or the increase in concentration of the products at constant temperature. For the heterogeneous reaction, however, the concept of concentration no longer has the same significance and the progress of reaction usually is determined in some other way. A kinetic study of heterogeneous reaction thus involves measurement of changes in mass or fraction reacted of the sample as a function of time at constant temperature [3,4,27]. Many equations relating the rate of solid-state reactions to are summarised in the literature. The interpretation of the kinetic equations is extremely complicated and considers the way in which the reaction starts, by a process of nucleation, then how those nuclei grow and what reaction or interface geometry is involved, and finally, how the reactants decay [6]. Nevertheless, in the developed our mathematical model, the fundamental kinetic equations for the homogeneous reactions are re-examined in an attempt to increase the reliability of the kinetic parameters obtained for solid-state reactions. Also, the validity of applying the Arrhenius equation to heterogeneous reactions has been questioned, but the parameters obtained had practical value even if their theoretical interpretation is difficult [7].

Developing a model we limit the analysis to the last stage of the YAG synthesis. At this stage the mass transport by diffusion, and the reaction are the limited phases of the YAG synthesis. Therefore the model is based on non-stationary diffusion equations (second Fick's law) containing a non-linear term related to the kinetics of the reaction (rate law). A crucial part of the model is the periodization of the reaction space of the YAG synthesis. It is used to locate the synthesis in the finite element (of clear form) of the reaction space. We propose several possible periodization models for the reaction space, which allow the simplification of the three-dimensional case of YAG synthesis model to one- and two-dimensional ones.

The models (i.e., systems of PDEs) were solved numerically in Sect. 4 of the article using finite difference techniques. Diferential problems were approximated by implicit schemes, and finite difference equations were solved using the sweep method.

The effectiveness of computer simulation depends very largely on input data precision. Solving the model we encountered the difficulties to determine precisely values

of some input parameters of the model. Namely, it turned out that the diffusion and reaction rate coefficents of the YAG synthesis are not known exactly so far, or they are indicated within the large scope and so cannot be used effectively for simulation. Such a situation caused a solution to this problem to be the main goal of our study. In the next section we present the literature overview concerning the methods of estimation of the diffusion and reaction rate coefficents. It should be noted that most of methods are of chemical nature, complicated enough, and/or expensive for realization. In Sect. 5 we have investigated in detail the problem appeared and proposed a method for calculation of the diffusion and reaction rate coefficents of the YAG synthesis. The method consists of three stages. Firstly, we analyze possible diffusion and reaction rates at fixed temperatures (1000 °C and 1600 °C). Using experimental data we solve the model and select the unknown input parameters of the YAG synthesis (diffusion and reaction rate coefficients) such that an output of the model (synthesis time) agrees with the experimental one. In such a way we get all possible values of the unknown parameters. Secondly, the analysis of the results prompted to investigation of some particular cases of the synthesis. Namely, we have distinguished and investigated in terms of the model developed following three cases:

(1) diffusion rate is infinite,
(2) reaction rate is infinite, and
(3) diffusion rate is sufficient.

As a result, classification of values of the diffusion and reaction rate coefficients has been introduced. Using the classification and experimental results we made conclusions and, as a result, locate values of the diffusion and reaction rate coefficients precisely enough. Finally, using simple calculations we presented expressions (Arrhenius laws) for the diffusion and reaction rate coefficients, which express the temperature dependence of the coefficients.

2 Experiments

We present in this section technical details and results (synthesis times and temperature regimes) of the experiments carried out by sol–gel and solid-state reaction methods.

2.1 Sol–gel method

In the sol–gel synthesis, yttrium oxide was dissolved in 150 mL of 0.2 mol L^{-1} CH_3COOH by stirring the mixture for 10 h at 55–60 °C in a beaker covered with a watch-glass. To this solution, aluminium nitrate dissolved in 50 mL of distilled water was added and the resulting mixture was stirred for 2 h at the same temperature. In a following step, 1.2 ethanediol (25 mmol) as complexing agent was added to the above solutions. The acidic medium (pH $\backsim$ 5) prevents the flocculation of metal hydroxides in the mixtures and no adjustment of pH was necessary. After concentrating the solutions by slow evaporation at 60–70 °C under stirring the Y–Al acetate–nitrate–glycolate solution turned into a white transparent gel. The oven dried (100–120 °C) gel became light brown due to the initial decomposition of nitrates. The gel powders

were ground in an agate mortar and preheated for 2 h at 800 °C in air. Since the gels are very combustible slow heating (2 °C min^{-1}) especially between 150 and 400 °C was found to be essential. After an intermediate grinding the powders were additionally sintered at various temperatures from 1000 to 1600 °C in air. The optimum annealing time was 8 h at 1000 °C and 4 h at 1600 °C.

2.2 Solid-state reaction method

In the solid-state reaction method, the stoichiometric mixture of metal oxides (Al_2O_3 and Y_2O_3) was carefully ground in an agate mortar and annealed at various temperatures from 1000 to 1600 °C in air. The monophasic YAG was obtained only at higher temperature, after sintering oxide precursor for 8 h at 1600 °C.

3 Mathematical model

The goal of this section is to construct a mathematical model of the YAG synthesis. We limit the analysis to the last stage of the synthesis, when the reactants, grounded and mixed thoroughly in the reaction space, react under high temperature. At this stage the mass transport by diffusion, and the reaction are the limited phases of the synthesis. The reaction is described by the following formula

$$3Y_2O_3 + 5Al_2O_3 \rightarrow 2Y_3Al_5O_{12}. \tag{1}$$

We treat the reaction space of the synthesis as a molecular structure, and assume that the reaction (1) could be considered as bimolecular

$$A + B \rightarrow C. \tag{2}$$

Such assumptions are quite reasonable since the temperature is high enough, and the reactants have been thoroughly mixed in the reaction space. The rate w_i of the reaction for the ith reactant is defined by

$$w_i = \frac{\partial c_i'}{\partial t}, \quad \text{where } c_i' \equiv \frac{c_i}{\gamma_i},\ i = 1, 2, 3, \tag{3}$$

where γ_i are the stoichiometric coefficients of the reaction (1), and $c_i = c_i(x, t)$ is the concentration of the ith reactant of the reaction at a point $x = (x_1, x_2, x_3)$ of the reaction space V at time t. Let $V \subset \mathbb{R}^3$ (see Fig. 1) is some cubic volume. The rate w of the reaction (2) is defined by

$$w = w_1 = w_2 = -w_3. \tag{4}$$

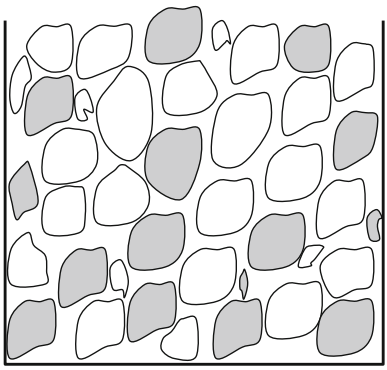

Fig. 1 Real chaotic structure of the reaction space V

Since the reaction (1) is considered as bimolecular, the reaction rate w could be expressed by rate law as follows

$$w = kc_1'c_2', \tag{5}$$

where k is a reaction rate constant.

The change of concentrations of the reactants by diffusion is described using the second Fick's law

$$\frac{\partial c_i'}{\partial t} = \sum_{j=1}^{3} D_i \frac{\partial^2 c_i'}{\partial x_j^2}, \tag{6}$$

where D_i is the diffusion coefficient of the ith reactant.

So, summarizing (3)–(6), the YAG synthesis can be described by the following reaction–diffusion system

$$\begin{aligned}
\frac{\partial c_1'}{\partial t} &= \sum_{j=1}^{3} D_1 \frac{\partial^2 c_1'}{\partial x_j^2} - kc_1'c_2', \\
\frac{\partial c_2'}{\partial t} &= \sum_{j=1}^{3} D_2 \frac{\partial^2 c_2'}{\partial x_j^2} - kc_1'c_2', \quad x \in V, \quad t > 0, \\
\frac{\partial c_3'}{\partial t} &= \sum_{j=1}^{3} D_3 \frac{\partial^2 c_3'}{\partial x_j^2} + kc_1'c_2',
\end{aligned} \tag{7}$$

or, using $c_i' \equiv \frac{c_i}{\gamma_i}$,

$$\frac{\partial c_1}{\partial t} = \sum_{j=1}^{3} D_1 \frac{\partial^2 c_1}{\partial x_j^2} - \frac{1}{5} k c_1 c_2,$$

$$\frac{\partial c_2}{\partial t} = \sum_{j=1}^{3} D_2 \frac{\partial^2 c_2}{\partial x_j^2} - \frac{1}{3} k c_1 c_2, \quad x \in V, \quad t > 0,$$

$$\frac{\partial c_3}{\partial t} = \sum_{j=1}^{3} D_3 \frac{\partial^2 c_3}{\partial x_j^2} + \frac{2}{15} k c_1 c_2, \tag{8}$$

The initial conditions ($t = 0$) for c_i are

$$c_i(x, 0) = c_i^0, \quad i = 1, 2, 3, \quad x \in \overline{V} = V \cup \partial V, \tag{9}$$

and the boundary conditions at ∂V are

$$\left.\frac{\partial c_i}{\partial x}\right|_{x \in \partial V} = 0, \quad i = 1, 2, 3, \quad t \geqslant 0. \tag{10}$$

The initial structure of the reaction space V, depicted in Fig. 1, is chaotic—exact initial position of particles of the reactants in V is unknown. So, it is quite reasonable to impose some conditions on V. In the following the periodization of the reaction space is used.

Let all particles are of same shape and its volume is small enough. More particularly, let particles are of the cube shape and the edge of the cube is $a\mu$m. Further, let these particles form a periodical structure (see Fig. 2, left part). It is easy to see that in such case the synthesis can be considered not in complete space, but only in its periodic part, i.e.

$$V = (0, a_1) \times (0, a_2) \times (0, a_3) \subset \mathbb{R}^3. \tag{11}$$

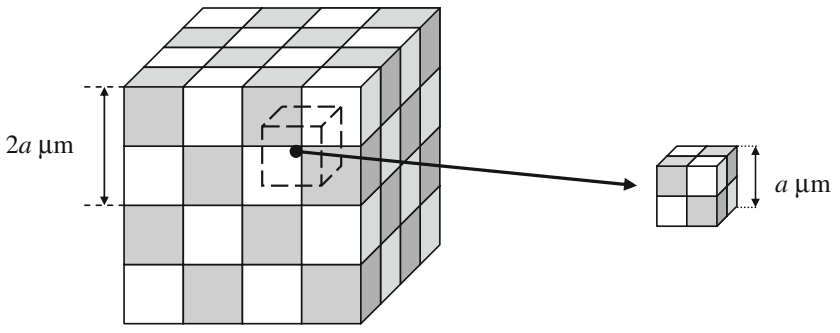

Fig. 2 Three-dimensional periodization model of the reaction space V

(See Fig. 2, right part.) From experimental data, a volume of the particle must be approximately $1\,\mu\text{m}^3$, sintering at 1000 °C using sol–gel method, and approximately $10\,\mu\text{m}^3$, sintering at 1600 °C using solid-state reaction method. So, in (11)

$$a_i = \begin{cases} 1, & \text{when } T = 1000\,^\circ\text{C}, \\ \sqrt[3]{10}, & \text{when } T = 1600\,^\circ\text{C}. \end{cases} \tag{12}$$

Let consider other possible periodization models of the reaction space V, which let us simplify calculations. Such cases are depicted in Fig. 3a and b.

- In case (a), $a_1 = 1,\ a_2 = 1,\ a_3 \gg 1$. Then the two-dimensional case of the model (8)–(10) can be considered

$$x = (x_1, x_2),$$
$$V = \begin{cases} \{x_1 : 0 \leqslant x_1 \leqslant 1,\ 0 \leqslant x_2 \leqslant 1\}, & \text{when } T = 1000\,^\circ\text{C}, \\ \{x_1 : 0 \leqslant x_1 \leqslant \sqrt{10},\ 0 \leqslant x_2 \leqslant \sqrt{10}\}, & \text{when } T = 1600\,^\circ\text{C}, \end{cases}$$

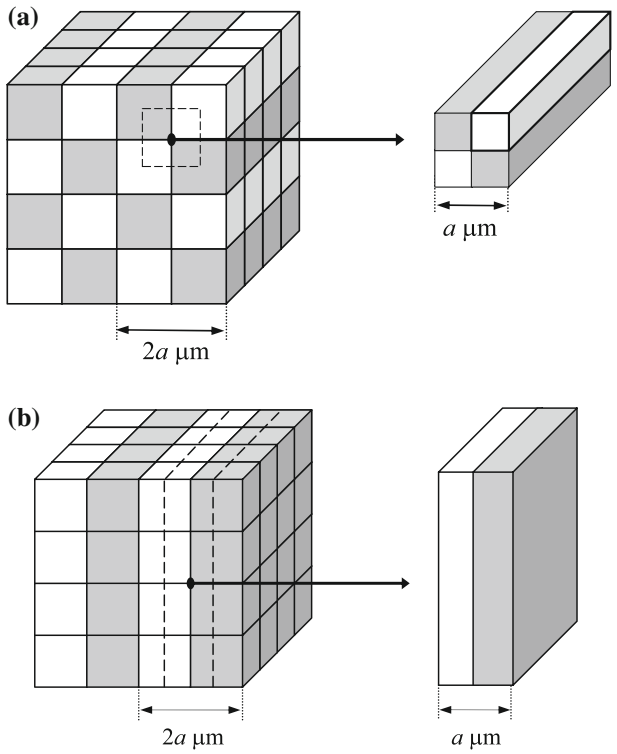

Fig. 3 Two-dimensional (**a**) and one-dimensional (**b**) periodization models of the reaction space V

- In case (b), $a_1 = 1,\ a_2, a_3 \gg 1$. Then the one-dimensional case of the model (8)–(10) can be considered

$$x = x_1,$$
$$V = \begin{cases} \{x_1 : 0 \leqslant x_1 \leqslant 1\}, & \text{when } T = 1000\,^\circ\text{C}, \\ \{x_1 : 0 \leqslant x_1 \leqslant 10\}, & \text{when } T = 1600\,^\circ\text{C}. \end{cases}$$

4 Numerical solution

We consider the problem:

$$\begin{aligned} \frac{\partial c_1}{\partial t} &= D_1 \frac{\partial^2 c_1}{\partial x^2} - \frac{1}{5} k c_1 c_2, \\ \frac{\partial c_2}{\partial t} &= D_2 \frac{\partial^2 c_2}{\partial x^2} - \frac{1}{3} k c_1 c_2, \quad x \in (0, a), \quad t > 0, \\ \frac{\partial c_3}{\partial t} &= D_3 \frac{\partial^2 c_3}{\partial x^2} + \frac{2}{15} k c_1 c_2, \end{aligned} \tag{13}$$

$$c_i(x, 0) = c_i^0, \quad i = 1, 2, 3, \quad x \in [0, a], \tag{14}$$

$$\left.\frac{\partial c_i}{\partial x}\right|_{x=0,\, x=a} = 0, \quad i = 1, 2, 3, \quad t \geqslant 0, \tag{15}$$

where

$$c_1^0 = \begin{cases} 3 \cdot 10^{-6}, & 0 \leqslant x \leqslant \frac{a}{2}, \\ 0, & \frac{a}{2} < x \leqslant a, \end{cases} \quad c_2^0 = \begin{cases} 0, & 0 \leqslant x \leqslant \frac{a}{2}, \\ 5 \cdot 10^{-6}, & \frac{a}{2} < x \leqslant a, \end{cases} \quad c_3^0 = 0.$$

and

$$a = \begin{cases} 1, & \text{kai } T = 1000\,^\circ\text{C}, \\ 10, & \text{kai } T = 1600\,^\circ\text{C}, \end{cases}$$

take $D_1 = D_2 = D_3 \equiv D$. Such assumption is quite reasonable since the size of the particles is small and similar.

The uniform grids were introduced in V

$$\omega_h = \{x_i : x_i = ih,\ i = 0, \ldots, N\}, \quad Nh = 1,$$
$$\omega_\tau = \{t^n : t^n = n\tau,\ n = 0, \ldots, M\}, \quad M\tau = T.$$

We use standard notation (see [37])

$$u_t = \frac{\left(u_i^{n+1} - u_i^n\right)}{\tau}, \quad u_{\bar{x}}^n = \frac{u_i^n - u_{i-1}^n}{h}, \quad u_x^n = \frac{u_{i+1}^n - u_i^n}{h},$$
$$u = u\left(x_i, t^n\right), \quad \hat{u} = u\left(x_i, t^{n+1}\right).$$

Define a discrete grid

$$\omega_{\tau,h} = \omega_\tau \times \omega_h = \left\{\left(t^n, x_i\right): t^n = n\tau,\ x_i = ih,\ i = 0, \ldots, N,\ n = 0, \ldots, M\right\}.$$

Let $u_{k,i}^n = u_k(x_i, t^n)$ be the lattice function defined at $\omega_{\tau,h}$ points. We build a finite difference scheme appoximating equations (13)

$$\begin{aligned} u_{1,t} &= \tfrac{1}{2} D\left(\hat{u}_{1,\bar{x}x} + u_{1,\bar{x}x}\right) - \tfrac{1}{5} k \hat{u}_{1,i} u_{2,i}, \\ u_{2,t} &= \tfrac{1}{2} D\left(\hat{u}_{2,\bar{x}x} + u_{2,\bar{x}x}\right) - \tfrac{1}{3} k \hat{u}_{1,i} \hat{u}_{2,i}, \\ u_{3,t} &= \tfrac{1}{2} D\left(\hat{u}_{3,\bar{x}x} + u_{3,\bar{x}x}\right) + \tfrac{2}{15} k \hat{u}_{1,i} \hat{u}_{2,i}, \end{aligned} \tag{16}$$

initial conditions (15)

$$u_{k,i}^0 = c_1^0, \quad k = 1, 2, 3,\ i = 0, \ldots, N, \tag{17}$$

and boundary conditions (14)

$$u_{k,0}^n = \varepsilon u_{k,1}^n, \quad u_{k,N}^n = \varepsilon u_{k,N-1}^n, \tag{18}$$

$$k = 1, 2, 3,\ n = 0, \ldots, M,\ \varepsilon = 1 - 10^{-6}. \tag{19}$$

Finite differrence scheme was solved using stream sweeping method [37]. We took

$$h = \begin{cases} 0.02 & \text{for } T = 1000\,^\circ\text{C}, \\ 0.2 & \text{for } T = 1600\,^\circ\text{C}, \end{cases} \quad \tau = 1.$$

A half-time $t_{1/2}$ is considered instead of the full synthesis time t_s, i.e. a time required for the half of the initial reactants to disappear:

$$\int_V \left(c_1(x, t_{1/2}) + c_2(x, t_{1/2})\right) dx = \frac{1}{2} \int_V \left(c_1(x, 0) + c_2(x, 0)\right) dx. \tag{20}$$

5 Calculation of diffusion and reaction rate coefficients

The effectiveness of computer simulation depends very largely on input data precision. In our case, the application of the model developed in previous sections is complicated in view of unknown input parameters—diffusion and reaction rate coefficients D and k. It turned out that the diffusion and reaction rate coefficients of the YAG synthesis are

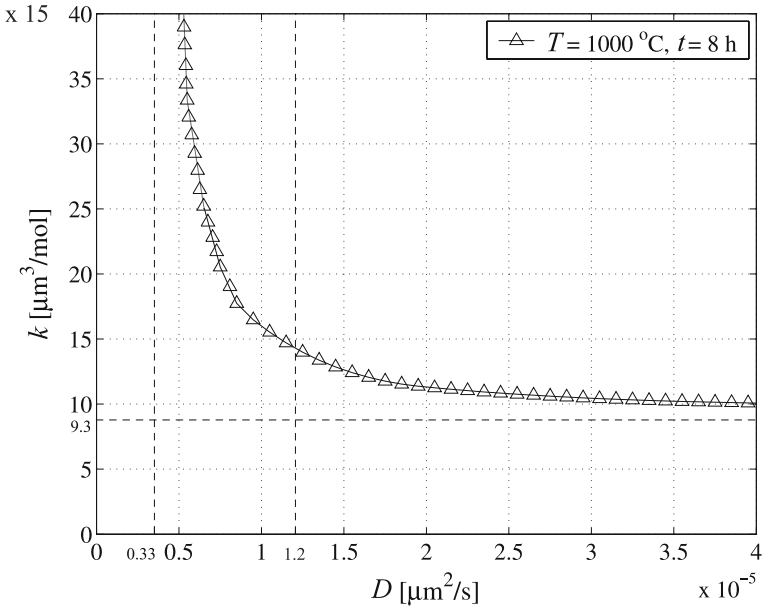

Fig. 4 Caculation of possible values of diffusion (D) and reaction (k) rate coefficients at 1000 °C. Solving the model with these input parameters D and k (△), an output of the model—synthesis time—agrees with the experimental one. The YAG phase was obtained after 8 h sintering at 1600 °C using solid-state reaction method and at 1000 °C using sol–gel method. Asymptotes $D = 3.3 \cdot 10^{-6}$ and $k = 138$ correspond to lower bounds of the parameters. When $D = 1.2 \cdot 10^{-5}$, reaction becomes the only limiting phase of the synthesis

not known exactly so far, or they are indicated within the large scope and so cannot be used effectively for simulation. Therefore alternative approach is investigated in this section and a method for calculation of the diffusion and reaction rate coefficients of the YAG synthesis is proposed. The inverse modelling problem is solved: using known experimental data—synthesis time, dimensions of reactants, etc.—the unknown input parameters of the model—diffusion and reaction rate coefficients—are calculated. The method consists of three stages.

First of all, we analyze possible diffusion and reaction rates at fixed temperatures (1000 and 1600 °C). Using experimental data we solve the model selecting the unknown input parameters of the YAG synthesis—diffusion and reaction rate coefficients—such that an output of the model—synthesis time—agrees with experimental data. Recall that the YAG phase was obtained after 8 h sintering at 1600 °C using solid-state reaction method and at 1000 °C using sol–gel method. Results of calculation at 1000 °C are presented in Fig. 4. In such a way we get all possible values of the unknown parameters. It is clear that different choice of pairs (D, k) causes different flow of the synthesis. Simulation experiments have prompted to investigation of some particular cases of the synthesis in more detail.

To begin with, we can find the lower bounds of diffusion and reaction rates, i.e. asymptotes of the curve in Fig. 4. For this we need to investigate limit cases of the model—when diffusion and reaction rates are infinite.

Assume that diffusion rate of the synthesis is infinite. The concentrations of reactants become constant in V instantly, so, in (13), $D\,\partial^2 c_i/\partial x^2 = 0$, and the problem (13)–(15) becomes:

$$\begin{aligned}
\frac{\partial c_1}{\partial t} &= -\frac{1}{5}kc_1c_2,\\
\frac{\partial c_2}{\partial t} &= -\frac{1}{3}kc_1c_2, \quad x \in (0,a), \quad t > 0,\\
\frac{\partial c_3}{\partial t} &= \frac{2}{15}kc_1c_2, \qquad (21)\\
c_i(x,0) &= \hat{c}_i^0, \quad i = 1,2,3, \quad x \in [0,a], \qquad (22)\\
\left.\frac{\partial c_i}{\partial x}\right|_{x=0,\,x=a} &= 0, \quad i = 1,2,3, \quad t \geqslant 0, \qquad (23)
\end{aligned}$$

and

$$\hat{c}_1^0 = \frac{3}{2}\cdot 10^{-6}, \quad \hat{c}_2^0 = \frac{5}{2}\cdot 10^{-6}, \quad \hat{c}_3^0 = 0.$$

The problem was solved numerically for different temperatures and k was chosen such that $t_{1/2} = 4$. We obtained

$$k_T^{\mathrm{a}} = 138,$$

for $T = 1000$ and $1600\,^\circ$C. It is obvious that such k_T^1 is the minimal value of the reaction rate, i.e. the YAG phase cannot be synthesized in 8 h if parameters D and k are selected from G_T^4 (see Fig. 5a, b) because of low reaction rate. In Fig. 5a and b this value corresponds to the line H.

Assume that reaction rate of the synthesis is infinite. The reaction proceeds instantly and reactants cannot pass through the reaction spot $x = a/2$ (introducing homogenous

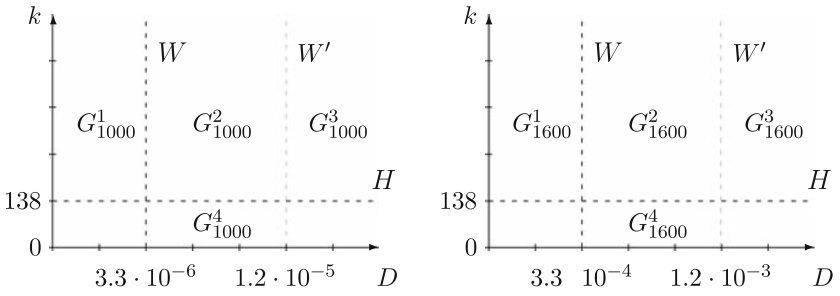

Fig. 5 Classification of values of diffusion (D) and reaction (k) rate coefficients

boundary condition), so, in (13), $c_1 c_2 = 0$, and the problem (13)–(15) becomes:

$$\frac{\partial c_1}{\partial t} = D\frac{\partial^2 c_1}{\partial x^2}, \quad x \in \left(0, \tfrac{a}{2}\right), \quad t > 0, \tag{24}$$

$$\frac{\partial c_2}{\partial t} = D\frac{\partial^2 c_2}{\partial x^2}, \quad x \in \left(\tfrac{a}{2}, a\right), \quad t > 0, \tag{25}$$

$$c_i(x, 0) = c_i^0, \quad i = 1, 2, \quad x \in [0, a], \tag{26}$$

$$\left.\frac{\partial c_1}{\partial x}\right|_{x=0} = 0, \quad \left.\frac{\partial c_2}{\partial x}\right|_{x=a} = 0, \quad c_i|_{x=\frac{a}{2}} = 0, \quad i = 1, 2, \quad t \geqslant 0. \tag{27}$$

Problem was solved numerically for different temperatures and D was chosen such that $t_{1/2} = 4$. We obtained

$$D^{\mathrm{l}}_{1000} = 3.3 \cdot 10^{-6} \quad \text{and} \quad D^{\mathrm{l}}_{1600} = 3.3 \cdot 10^{-4}.$$

It is obvious that such D^{l}_T is the minimal value of the diffusion rate, i.e. the YAG phase cannot be synthesized in 8 h if parameters D and k are selected from G^{l}_T (see Fig. 5a, b) because of low diffusion rate. In Fig. 5a and b these values correspond to the line W.

At the same time, the following conclusion follows. The difference between D^{l}_{1000} and D^{l}_{1600} explains the low-temperature formation of $Y_3Al_5O_{12}$ using sol–gel technique: since sol–gel method requires lower diffusion rate, it may be caried out at lower-temperature regime.

Now, let us consider diffusion separately. Let us define "sufficient" diffusion rate of the YAG synthesis. In other words, we look for a value of diffusion rate at which diffusion is no longer the limited stage of the synthesis. It is not difficult to understand that such diffusion guarantees the delivery of the reactants to the reaction spot over 8 h exactly. in the following system

$$\frac{\partial c_i}{\partial t} = D\frac{\partial^2 c_i}{\partial x^2}, \quad i = 1, 2, \quad x \in (0, a), \quad t > 0, \tag{28}$$

$$c_i(x, 0) = c_i^0, \quad i = 1, 2, \quad x \in [0, a], \tag{29}$$

$$\left.\frac{\partial c_i}{\partial x}\right|_{x=0,\, x=a} = 0, \quad i = 1, 2, \quad t \geqslant 0. \tag{30}$$

the parameter D should be selected such that

$$\int_{V_1^0} c_1(x, t_{\mathrm{s}}) + \int_{V_2^0} c_2(x, t_{\mathrm{s}})\, dx = \frac{1}{2}\int_V \big(c_1(x, 0) + c_2(x, 0)\big)\, dx, \tag{31}$$

$$V_i^0 = \big\{x : c_i(x, 0) = 0\big\}, \quad i = 1, 2, \quad t_{\mathrm{s}} = 8 \text{ val}. \tag{32}$$

Problem was solved numerically for different temperatures. We obtained

$$D^{s}_{1000} = 1.2 \cdot 10^{-5} \quad \text{and} \quad D^{s}_{1600} = 1.2 \cdot 10^{-3}.$$

in Fig. 5a and b these values correspond to line W'.

As a result, classification of values of the diffusion and reaction rate coefficients has been introduced—see Fig. 5. According to experimental observations, diffusion and reaction both are limiting stages of the synthesis, and therefore the coefficients should be taken from G^2_T areas. These areas are not wide, and values could be chosen freely, but in fact there is a possibility to choose these values at 1600 °C more strictly. Recall that we have experimental results at 1600 °C of the synthesis by solid-state reaction and sol–gel methods. We can calculate all possible D, k values using the model, and the point of intersection of the curves obtained will be the values for the coefficients needed. The results are presented in Fig. 6. We obtained

$$D_{1600} = 8 \cdot 10^{-4} \quad \text{and} \quad k_{1600} = 280.095.$$

At 1000 °C we take

$$D_{1000} = 10^{-5} \quad \text{and} \quad k_{1000} = 234.105.$$

Our final task is to find the formulas which express the temperature dependence of the diffusion and reaction rate coefficients. It may be described by the following

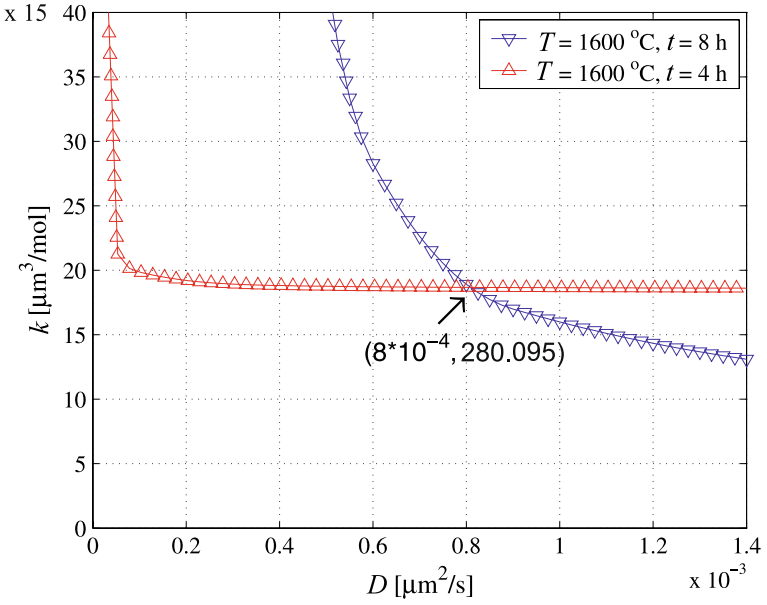

Fig. 6 Diffusion and reaction coefficients at 1600 °C

Arrhenius laws:

$$D = D_0 \exp\left(-\frac{E_D}{RT}\right), \quad k = k_0 \exp\left(-\frac{E_k}{RT}\right), \tag{33}$$

where E_D, E_k—activation energies for diffusion and reaction; D_0, k_0, $R = 8.314472$ —constants. We need to calculate constants E_D, E_k and D_0, k_0.

Let write expressions (33) for $T = 1000\,^{\circ}\mathrm{C}$ and $T = 1600\,^{\circ}\mathrm{C}$

$$D_{1000} = D_0 \exp\left(-\frac{E_D}{R \cdot 1273}\right), \quad k_{1000} = k_0 \exp\left(-\frac{E_k}{R \cdot 1273}\right), \tag{34}$$

$$D_{1600} = D_0 \exp\left(-\frac{E_D}{R \cdot 1873}\right), \quad k_{1600} = k_0 \exp\left(-\frac{E_k}{R \cdot 1873}\right). \tag{35}$$

Recall that we have D_{1000}, D_{1600} and k_{1000}, k_{1600}. Dividing D_{1000}/D_{1600} and k_{1000}/k_{1600}, we eliminate D_0, k_0 and calculate constants E_D, E_k. Then return to (34), (35) and calculate D_0, k_0. So, we obtained

$$D = 8.73 \exp\left(-\frac{144785}{RT}\right), \quad k = 409.5 \exp\left(-\frac{5917.76}{RT}\right).$$

References

1. T. Aichele, T. Lorenz, R. Hergt, P. Gornert, Cryst. Res. Technol. **38**, 575 (2003)
2. J.L. Bates, J.E. Garnier, J. Am. Ceram. Soc. **64**, C-138 (1981)
3. M.E. Brown, *Introduction to Thermal Analysis. Techniques and Applications* (Chapman and Hall, London, 1988)
4. G.W. Chadzynski, V.V. Kutarov, P. Staszczuk, J. Therm. Anal. Calorim. **76**, 633 (2004)
5. J. Dong, P. Deng, J. Xu, Optics Commun. **170**, 255 (1999)
6. J.R. Frade, M. Cable, J. Mater. Sci. **32**, 2727 (1997)
7. A.K. Galwey, M.E. Brown, Thermochim. Acta **386**, 91 (2002)
8. E. Garskaite, D. Jasaitis, A. Kareiva, J. Serb. Chem. Soc. **68**, 677 (2003)
9. J. George, G. Varghese, Liesegang patterns: estimation of diffusion coefficient and a plausible justification for colloid explanation. Colloid Polym. Sci. **280**(12), 1131–1136 (2002)
10. Q.Z. Guo, V.R. Subramanian, J.W. Weidner, R.E. White, Estimation of diffusion coefficient of lithium in carbon using AC impedance technique. J. Electrochem. Soc. **149**(3), A307–A318 (2002)
11. C.J. Harlan, A. Kareiva, D.B. Macqueen, R. Cook, A.R. Barron, Adv. Mater. **9**, 68 (1997)
12. W.P. Hsu, P.Y. Lo, T.K. Kwei, A.S. Myerson, Parameter-estimation for analysis of vapor diffusion in polymers. Polym. Eng. Sci. **34**(16), 1250–1253 (1994)
13. A. Ikesue, K. Yoshida, K. Kamata, J. Am. Ceram. Soc. **79**, 507 (1996)
14. S.M. Kaczmarek, G. Domianiak-Dzik, W. Ryba-Romanowski, J. Kisielewski, J. Wojtkowska, Cryst. Res. Technol. **34**, 1031 (1999)
15. B.H. King, J.W. Halloran, J. Am. Ceram. Soc. **78**, 2141 (1995)
16. A. Leleckaite, A. Kareiva, Opt. Mater. **26**, 123 (2004)
17. Y. Liu, Z.F. Zhang, B. King, J. Halloran, R.M. Laine, J. Am. Ceram. Soc. **79**, 385 (1996)
18. M. Malinowski, M. Kaczkan, A. Wnuk, M. Szufliska, J. Lumin. **106**, 269 (2004)
19. R. Manalert, M.N. Rahaman, J. Mater. Sci. **31**, 3453 (1996)
20. M. Mourad, M. Hemati, C. Laguerie, A new correlation for the estimation of moisture diffusivity in corn kernels from drying kinetics. Drying Technol. **14**(3–4), 873–894 (1996)

21. I. Muliuoliene, S. Mathur, D. Jasaitis, H. Shen, V. Sivakov, R. Rapalaviciute, A. Beganskiene, A. Kareiva, Opt. Mater. **22**, 241 (2003)
22. R.C. Pullar, M.D. Taylor, A.K. Bhattacharya, J. Eur. Ceram. Soc. **19**, 1747 (1999)
23. R.V.G. Rao, U. Bandyopadhyay, R. Venkatesh, A new approach in the estimation of diffusion-coefficient and its pressure derivative in liquids. Physica Status Solidi B-Basic Res. **181**(1), K1–K5 (1994)
24. A.A. Samarskij, *Theory of Finite Difference Schemes* (Dekker, 2002)
25. Z. Sun, D. Yuan, H. Li, X. Duan, H. Sun, Z. Wang, X. Wei, H. Xu, C. Luan, D. Xu, M. Lv, J. All. Comp. **379**, L1 (2004)
26. H. Takaba, T. Suzuki, S. Nakao, Estimation of diffusion coefficient and permeance of aromatic molecules in silicalite and MgZSM-5 using quantum calculation and dynamic Monte Carlo simulation. Fluid Phase Equilib. **219**(1), 11–18 (2004)
27. H. Tanaka, Thermochim. Acta **267**, 29 (1995)
28. N. Tantemsapya, J.N. Meegoda, Estimation of diffusion coefficient of chromium in colloidal silica using digital photography. Environ. Sci. Technol. **38**(14), 3950–3957 (2004)
29. C.W. Thiel, H. Cruguel, Y. Sun, G.J. Lapeyre, R.M. Macfarlane, R.W. Equall, R.L. Cone, J. Lumin. **94–95**, 1 (2001)
30. T. Tsuda, S. Kitagawa, T. Ono, M. Maeda, Novel instrumentation for measurement of diffusion coefficient by capillary zone electrophoresis and its application to aqua lanthanide ions. J. Capillary Electrophor. **4**(3), 113–116 (1997)
31. N. Vahdat, Estimation of diffusion-coefficient for solute polymer systems. J. Appl. Polym. Sci. **42**(12), 3165–3171 (1991)
32. M. Veith, S. Mathur, A. Kareiva, M. Jilavi, M. Zimmer, V. Huch, J. Mater. Chem. **9**, 3069 (1999)
33. S. Vyazovkin, C.A. Wight, Ann. Rev. Physic. Chem. **48**, 125 (1997)
34. S.F. Wuister, C.D. Donega, A. Meijerink, Phys. Chem. Chem. Phys. **6**, 1633 (2004)
35. M. Yada, M. Ohya, M. Machida, T. Kijima, Chem. Commun. 1941 (1998)
36. J.M. Yang, S.M. Jeng, S. Chang, J. Am. Ceram. Soc. **79**, 1218 (1996)
37. X. Zhang, H. Liu, W. He, J. Wang, X. Li, R.I. Boughton, J. All. Comp. **372**, 300 (2004)